

# Achilles tendon and enthesis assessment using ultrashort echo time magnetic resonance imaging (UTE-MRI) T1 and magnetization transfer (MT) modeling in psoriatic arthritis

Dina Moazamian<sup>1</sup>  | Jiyo S. Athertya<sup>1</sup>  | Sophia Dwek<sup>1</sup> |  
 Alecio F. Lombardi<sup>1</sup>  | Hamidreza Shaterian Mohammadi<sup>1</sup> | Sam Sedaghat<sup>1,2</sup> |  
 Hyungseok Jang<sup>1</sup> | Yajun Ma<sup>1</sup> | Christine B. Chung<sup>1,3</sup> | Jiang Du<sup>1,3</sup> |  
 Saeed Jerban<sup>1,3,4</sup> | Eric Y. Chang<sup>1,3</sup>

<sup>1</sup>Department of Radiology, University of California, San Diego, California, USA

<sup>2</sup>Department of Diagnostic and Interventional Radiology, University Hospital Heidelberg, Heidelberg, Germany

<sup>3</sup>Radiology Service, VA San Diego Healthcare System, San Diego, California, USA

<sup>4</sup>Department of Orthopedic Surgery, University of California, San Diego, California, USA

## Correspondence

Eric Y. Chang, VA San Diego Healthcare System, San Diego, CA 92161, USA.  
 Email: [eric.chang2@va.gov](mailto:eric.chang2@va.gov)

Saeed Jerban and Dina Moazamian, Department of Radiology, University of California, San Diego, 9500 Gilman Drive, La Jolla, CA 92093, USA.  
 Email: [sjerban@health.ucsd.edu](mailto:sjerban@health.ucsd.edu) and [dmoazamian@health.ucsd.edu](mailto:dmoazamian@health.ucsd.edu)

## Funding information

National Institutes of Health, Grant/Award Numbers: R01AR075825, R01AR068987, R01AR062581, K01AR080257, R01AR079484, 5P30AR073761, R01AR078877; U.S. Department of Veterans Affairs, Grant/Award Numbers: I01CX001388, 1I01BX005952, I01CX000625; GE Healthcare

## Abstract

The purpose of this study is to investigate the use of ultrashort echo time (UTE) magnetic resonance imaging (MRI) techniques (T1 and magnetization transfer [MT] modeling) for imaging of the Achilles tendons and entheses in patients with psoriatic arthritis (PsA) compared with asymptomatic volunteers. The heels of twenty-six PsA patients (age  $59 \pm 15$  years, 41% female) and twenty-seven asymptomatic volunteers (age  $33 \pm 11$  years, 47% female) were scanned in the sagittal plane with UTE-T1 and UTE-MT modeling sequences on a 3-T clinical scanner. UTE-T1 and macromolecular proton fraction (MMF; the main outcome of MT modeling) were calculated in the tensile portions of the Achilles tendon and at the enthesis (close to the calcaneus bone). Mann-Whitney-U tests were used to examine statistically significant differences between the two cohorts. UTE-T1 in the entheses was significantly higher for the PsA group compared with the asymptomatic group ( $967 \pm 145$  vs.  $872 \pm 133$  ms,  $p < 0.01$ ). UTE-T1 in the tendons was also significantly higher for the PsA group ( $950 \pm 145$  vs.  $850 \pm 138$  ms,  $p < 0.01$ ). MMF in the entheses was significantly lower in the PsA group compared with the asymptomatic group ( $15\% \pm 3\%$  vs.  $18\% \pm 3\%$ ,  $p < 0.01$ ). MMF in the tendons was also significantly lower in the PsA group compared with the asymptomatic group ( $17\% \pm 4\%$  vs.  $20\% \pm 5\%$ ,  $p < 0.01$ ). Percentage differences in MMF between the asymptomatic and PsA groups ( $-16.6\%$  and  $-15.0\%$  for the enthesis and tendon, respectively) were higher than the T1 differences ( $10.8\%$  and  $11.7\%$  for the enthesis and tendon, respectively). The results suggest higher T1 and lower MMF in the Achilles tendons and entheses in PsA patients compared with the asymptomatic group. This study highlights the potential of UTE-T1 and UTE-MT modeling for quantitative evaluation of entheses and tendons in PsA patients.

## KEYWORDS

Achilles tendon, enthesis, MRI, Psoriatic Arthritis, UTE-MRI

**Abbreviations:** 2D, two-dimensional; 3D-UTE, three-dimensional ultrashort echo time; AFI-VFA, actual flip angle-variable flip angle; FA, flip angle; FOV, field of view; FSE, fast-spin echo; MMF, macromolecular proton fraction; MRI, magnetic resonance imaging; MTR, magnetization transfer ratio; PD, proton-density; PsA, psoriasis arthritis; qMRI, quantitative magnetic resonance imaging; RF, radiofrequency; ROI, region of interest; SpA, spondyloarthropathies; TE, echo time; TR, repetition time; US, ultrasound.

## 1 | INTRODUCTION

Entheses are regions that connect tendons, ligaments, and joint capsules to bone.<sup>1</sup> Enthesitis is considered an important pathophysiological feature of spondyloarthropathies (SpA), particularly psoriatic arthritis (PsA).<sup>2</sup> Because enthesitis can represent a primary lesion in PsA, and in particular manifesting in the Achilles tendon, early detection can help in the timely diagnosis of PsA.<sup>3-5</sup> Clinical assessment of the entheses lacks sensitivity and specificity because of the deeper location, proximity to other pain generators such as the synovium, and a highly heterogeneous composition and structure.<sup>5-8</sup> Unfortunately, diagnosis failure can lead to treatment delays and long-term consequences.

With the advantages of modern imaging modalities such as ultrasound (US) and magnetic resonance imaging (MRI), the diagnosis of PsA has improved, and monitoring after the implementation of treatment strategies has been enhanced.<sup>5</sup> US can be used to visualize the entheses, but it is operator dependent, and robust quantitative assessments are lacking.<sup>5,6</sup> Conventional MRI techniques such as T1-weighted and T2-weighted fat-suppressed fast-spin echo (FSE) sequences can demonstrate morphological changes of the Achilles tendon and entheses when grossly abnormal. Quantitative MRI (qMRI) biomarkers such as T1, magnetization transfer ratio (MTR), and T2\* can provide valuable information about the microstructural and compositional changes in PsA-affected tissues without requiring high spatial resolutions.<sup>9-11</sup> The presence of edema, inflammation, fibrosis, and tissue erosion are common features of PsA that involve microstructural and compositional changes.<sup>11-13</sup> However, intact tendons and entheses, as well as fibrotic tissues, have short T2s and show little or no signal, which limits their ability to be quantified by routine qMRI.<sup>7,8</sup>

Ultrashort echo time (UTE) MRI sequences use echo times (TEs) that are 100–1000 times shorter than those in clinical sequences, which allows direct imaging of traditionally MRI “invisible” tissues, such as tendons and entheses.<sup>14,15</sup> The high signal obtained with UTE-MRI can also be used to perform quantitative assessments. There has been increasing interest in recent years in the use of UTE-MRI for the evaluation of the Achilles tendon and its entheses, both morphologically and quantitatively.<sup>13,16-18</sup>

Hodgson et al. used a two-dimensional (2D) UTE sequence before and after gadolinium administration to evaluate the signal intensity of the Achilles tendons in patients with SpA. They reported significantly higher signal enhancement in the entheses of SpA patients compared with healthy controls.<sup>17</sup> The same authors also employed a quantitative 2D UTE magnetization transfer (MT) technique to assess the Achilles tendon in one patient with PsA compared with eight asymptomatic volunteers. In the patient with PsA, they showed that the “bound proton fraction” which was generated from MT modeling and assumed to represent the macromolecular contents of tissues, was 16.4% lower than that of the asymptomatic volunteers.<sup>18</sup> Chen et al. used a three-dimensional (3D) Cones UTE sequence and demonstrated significantly higher T2\* values and lower MTRs in the Achilles tendons and entheses of patients with PsA compared with the healthy control group.<sup>13</sup> Notably, T2\* is sensitive to the magic angle effect<sup>14</sup> and may differ significantly only due to changes in the tissue direction relative to the B<sub>0</sub> field. On the other hand, MTR values are difficult to interpret because of dependence on both the underlying physiology and the acquisition parameters (e.g., pulse power level, pulse duration, and frequency offsets).<sup>18</sup> Chen et al. also used UTE-MT modeling to evaluate normal cadaveric Achilles tendons and entheses and showed lower macromolecular proton fraction (MMF) values in the entheses compared with the tensile tendon regions.<sup>16</sup> UTE-MT modeling provides a magic angle insensitive evaluation of water and MMF in short T2 tissues.<sup>14,19</sup> Because T1 relaxation impacts the magnetization saturation in the macromolecular pool and the transferred saturation to the water proton pools, using a correct T1 value is necessary for accurate estimation of MMF in the UTE-MT modeling technique. The utilization of UTE-MT modeling in the evaluation of the Achilles tendons and entheses and distinguishing between PsA patients and asymptomatic volunteers remains to be investigated.

In the present study, we aim to evaluate the Achilles tendons and entheses in asymptomatic volunteers and PsA patients using 3D UTE-Cones sequences at 3 T. Quantitative measurements of T1 and MMF of the Achilles tendons and entheses were measured for each subject, and differences were analyzed between the two groups.

## 2 | MATERIALS AND METHODS

### 2.1 | Subjects

This cross-sectional study was approved by our institutional review board, and written informed consent was obtained from all subjects. From September 2021 to December 2022, adult participants aged 19–90 years without a history of trauma to the ankle, were recruited. The asymptomatic cohort consisted of volunteers from the University campus with no ankle symptoms of any sort. The PsA cohort consisted of consecutive patients referred from our rheumatology clinic with a diagnosis of PsA, as established by the standard, validated classification for Psoriatic Arthritis (CASPAR) criteria.<sup>20,21</sup> Participants with image artifacts that could not be corrected were excluded.

## 2.2 | Image acquisition

A 3-T clinical scanner (MR750, GE Healthcare Technologies, Milwaukee, WI, USA) employing a 7.6 cm. surface coil was used. The ankles of the participants were scanned in the sagittal plane using quantitative 3D UTE-T1 and 3D UTE-MT sequences with a Cones k-space trajectory, as well as with conventional clinical 2D proton-density (PD) and T2-weighted fat-suppressed FSE sequences. The quantitative 3D UTE-T1 sequence is based on the 3D-UTE actual flip angle-variable flip angle (AFI-VFA) method.<sup>15</sup> UTE-MT modeling requires T1 compensation as a short TR to reduce the total scan time.<sup>15</sup>

The detailed sequence parameters of the quantitative 3D-UTE imaging protocols and conventional clinical MRI were: (A) 3D UTE-AFI-VFA sequence: TE = 0.032 ms, TR = 18 ms, flip angles (FAs) = 5°, 12°, and 24°; (B) 3D-UTE-Cones-MT sequence: pulse power = 350°, 750°; frequency offset = 2, 5, 10, 20, and 50 kHz; FA = 7°; 11 spokes per MT preparation; slice spacing/thickness = 2.0 mm, field of view (FOV) = 12 × 12 cm<sup>2</sup>, matrix size = 256 × 256; (C) 2D sagittal fat saturation T2-weighted FSE images were acquired with TE = 70 ms, TR = 4713 ms, slice spacing/thickness = 2.0 mm, FOV = 12 × 12 cm<sup>2</sup>, matrix size = 352 × 256, receiver bandwidth = 162 kHz; and (D) 2D sagittal PD-weighted images were acquired with TE = 31.9 ms, TR = 2000 ms, slice spacing/thickness = 2.0 mm, FOV = 12 × 12 cm<sup>2</sup>, and matrix size = 352 × 256. The total scan time was 23 min 5 s.

## 2.3 | Image/data analysis

For each patient, motion registration was performed using the Elastix software (<https://elastix.lumc.nl/>) based on the well-known Insight Segmentation and Registration Toolkit [ITK]. Specifically, a rigid, affine transformation was applied for coarse registration between images, followed by a nonrigid b-spline registration for more accurate registration.<sup>22</sup>

An experienced postdoctoral scholar, blinded to the patient group and clinical data, performed the data analysis using MATLAB (2022; MathWorks, MA, USA). Quantitative UTE analysis was performed on two sagittal slices 3 mm apart. On each slice, two different regions of interest (ROIs) were selected, including one in the tensile portion of the Achilles tendon and one in the enthesis (close to the calcaneus bone) (Figure 1D). For the selection of the ROIs, the tendon was approximated into deep and superficial halves by the readers. To avoid potential partial

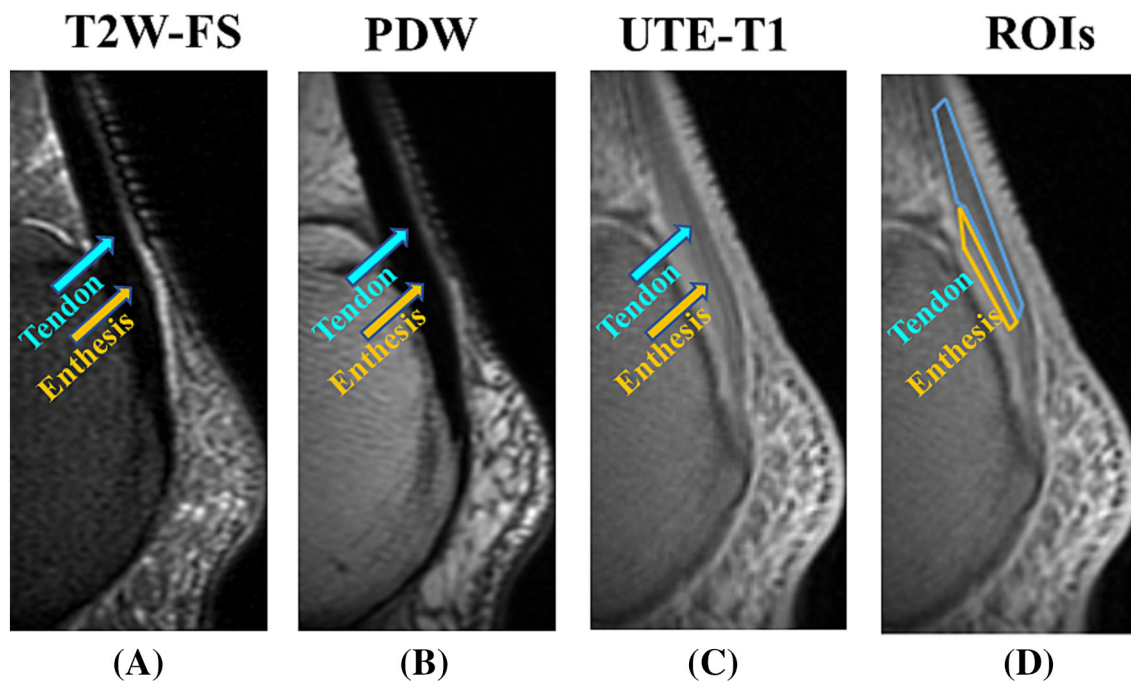


**FIGURE 1** (A) T2-weighted fat-suppressed (T2W-FS), (B) Proton-density weighted (PDW), and (C) UTE-T1 images of the ankle for an asymptomatic 35-year-old male volunteer. Note that the Achilles tendon (blue arrow) and enthesis (yellow arrow) show no signal on conventional clinical MRI images (A and B). On the UTE-T1 image, the enthesis is evident as a region with a higher signal between the Achilles tendon and calcaneus (C). Using the UTE-T1 image, schematic ROIs were placed in the tensile tendon (blue polygon) and enthesis (yellow polygon) for measurement, as shown (D). For the selection of the ROIs, the tendon was approximated into deep and superficial halves by the readers. To avoid potential partial volume artifacts with structures of vastly different structure and composition, the selected ROIs for the entheses avoided the hypointense calcaneal cortex and immediately superficial, but variably hyperintense, fibrocartilage. ROI, region of interest; UTE, ultrashort echo time.

volume artifacts with structures of vastly different structures and compositions, the selected ROIs for the entheses avoided the hypointense calcaneal cortex and immediately superficial, but variably hyperintense, fibrocartilage. T1 measurements were performed using a single-component exponential fitting model based on a Levenberg–Marquardt algorithm using nonlinear optimization.<sup>23</sup> Two-pool MT modeling, which relies on the interaction between water and macromolecular protons, was performed to generate MMF values. In this technique, by selectively saturating the macromolecular proton pool using off-resonance radiofrequency pulses, magnetization is transferred to the water proton pool, resulting in a decrease in signal intensity that can be used to study these interactions.<sup>14</sup> T1 and MMF mean values, standard deviation, and fitting errors were recorded for each subregion. Spearman's correlation coefficient was calculated to evaluate the relationship between MFF and T1 values.

A second experienced postdoctoral scholar, also blinded to the patient group and clinical data and the results from the first postdoctoral scholar, performed data analysis similarly for all the participants to assess inter-rater reliability. One asymptomatic volunteer was scanned with the same protocol and scanner three times to assess repeatability.

## 2.4 | Statistical analysis

SPSS (IBM, Armonk, NY, USA) version 28.0 was used for all statistical analyses. The 3D UTE-T1 and MMF values in the Achilles tendons and entheses were compared between the asymptomatic volunteers and the PsA groups. The Kolmogorov–Smirnov test was used to examine whether the 3D UTE-Cones T1 and MMF values were normally distributed. The Mann–Whitney-U test (because they were not normally distributed) was used to examine the differences and their statistical significance between asymptomatic volunteers and PsA groups. To evaluate the inter-reader reliability and validity, intraclass correlation coefficients (ICCs) were calculated between the results of the two analyzers. To assess intra-reader reliability, ICCs were calculated between the results of the 10 randomly selected participants. To evaluate the test–retest reliability study, ICCs were calculated for the results of the one asymptomatic volunteer. *p* values less than 0.05 were considered statistically significant.

## 3 | RESULTS

Twenty-six asymptomatic volunteers and 27 patients diagnosed with PsA were recruited. However, because of severe motion artifacts that could not be resolved with retrospective motion correction, our final cohorts consisted of 20 patients with PsA (age  $59 \pm 15$  years, 41% female) and 25 asymptomatic volunteers (age  $33 \pm 11$  years, 47% female).

T1 and MMF pixel maps of two representative PsA patients and two asymptomatic volunteers in Figure 2A (a-f) and Figure 2B (c-h), respectively. The mean and standard deviation of UTE-T1 and MMF values in PsA and asymptomatic volunteer groups are presented in Table 1. The mean and standard deviation of T1 values in the entheses for PsA patients and the asymptomatic volunteer group were  $967 \pm 145$  versus

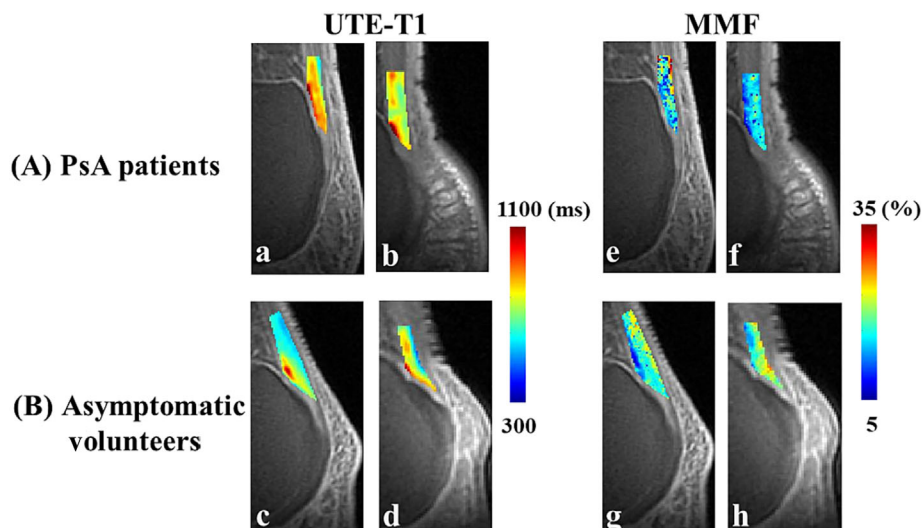


**FIGURE 2** Representative UTE-T1 and MMF pixel maps overlaid onto the UTE images in (A) Two PsA patients, and (B) Two young asymptomatic volunteers. A higher mean value of T1 was observed for the PsA patients (a and b) compared with the volunteers (c and d) in both entheses ( $967 \pm 145$  vs.  $872 \pm 133$  ms) and Achilles tendon ( $950 \pm 145$  vs.  $850 \pm 138$  ms). A lower mean value of MMF (%) was observed for the PsA patients (e and f) compared with the volunteers (g and h) in both entheses ( $15\% \pm 3\%$  vs.  $18\% \pm 3\%$ ) and Achilles tendon ( $17\% \pm 4\%$  vs.  $20\% \pm 5\%$ ). MMF, macromolecular proton fraction; PsA, psoriatic arthritis; UTE, ultrashort echo time.

**TABLE 1** Mean and standard deviation of UTE-T1 (ms) and MMF (%) measures in patients with PsA and the asymptomatic group.

ROI	Groups	T1 (ms)	MMF (%)
Enthesis	PsA patients	967 ± 145	15 ± 3
	Asymptomatic	872 ± 133	18 ± 3
Tendon	PsA patients	950 ± 145	17 ± 4
	Asymptomatic	850 ± 138	20 ± 5

Abbreviations: MMF, macromolecular proton fraction; PsA, psoriatic arthritis; ROI, region of interest; UTE, ultrashort echo time.

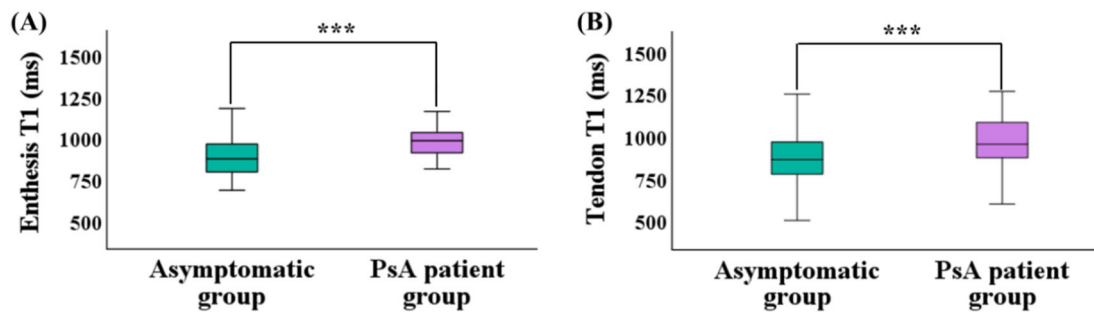


**FIGURE 3** (A) Bar-plot of the entheses T1 (ms) values comparing between asymptomatic and PsA groups ( $***p < 0.01$ ). (B) Bar-plot of the Achilles tendon T1 (ms) comparing between asymptomatic and PsA groups ( $***p < 0.01$ ). The central line in each plot indicates the median value, while the bottom and top edges of the box indicate the 25th and 75th percentiles, respectively. Enthesis and the Achilles tendon in PsA patients showed significantly higher T1 values compared with the asymptomatic group (967 ± 145 vs. 872 ± 133 ms for entheses, while 950 ± 145 vs. 850 ± 138 ms for the tensile tendon region). PsA, psoriatic arthritis.

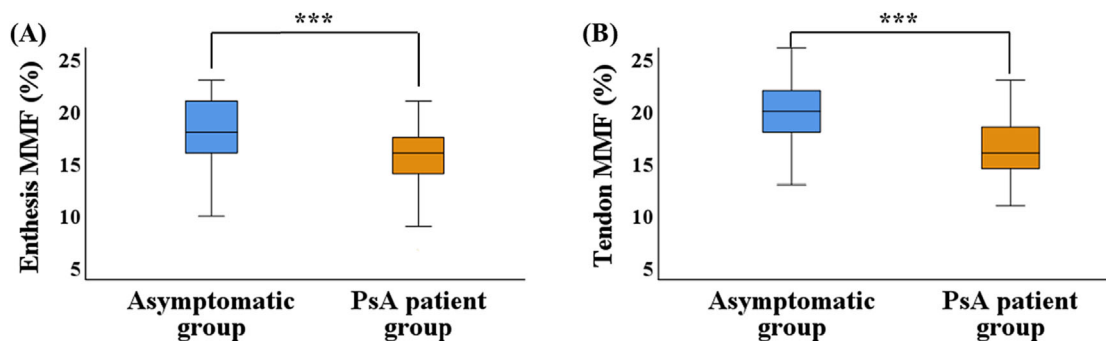


**FIGURE 4** (A) Bar-plot of the entheses MMF (%) values comparing between asymptomatic and PsA groups ( $***p < 0.01$ ). (B) Bar-plot of the Achilles tendon MMF (%) comparing between asymptomatic and PsA groups ( $***p < 0.01$ ). The central line in each plot indicates the median value, while the bottom and top edges of the box indicate the 25th and 75th percentiles, respectively. Enthesis and the Achilles tendon in PsA patients showed significantly lower MMF values compared with the asymptomatic group (15% ± 3% vs. 18% ± 3% for entheses, while 17% ± 4% vs. 20% ± 5% for the tensile tendon region). MMF, macromolecular proton fraction; PsA, psoriatic arthritis.

872 ± 133 ms, respectively ( $p < 0.01$ ) (Figure 3A). The mean and standard deviation values of T1 values in the tensile tendon were 950 ± 145 versus 850 ± 138 ms for PsA patients and the asymptomatic volunteer group, respectively ( $p < 0.01$ ) (Figure 3B). The mean and standard deviation of MMF values in the entheses for PsA patients and the asymptomatic volunteer group were 15% ± 3% versus 18% ± 3%, respectively ( $p < 0.01$ ) (Figure 4A). The mean and standard deviation of MMF values in the tensile tendon for PsA patients and the asymptomatic volunteer group were 17% ± 4% versus 20% ± 5%, respectively ( $p < 0.01$ ) (Figure 4B).

Percentage differences and the statistical significance of T1 values between PsA groups and asymptomatic volunteers in the entheses and the tensile tendon regions were 10.8% ( $p < 0.01$ ) and 11.7% ( $p < 0.01$ ), respectively. For MMF, there were significant percentage differences of -16.6% ( $p < 0.01$ ) and -15.0% ( $p < 0.01$ ) between the PsA groups and asymptomatic volunteers in the entheses and the tensile tendon regions,

**TABLE 2** Percentage differences and their statistical significance (Mann–Whitney-U) in UTE-T1 (ms) and MMF (%) measures between patients with PsA and the asymptomatic group.

	Diff T1 (%)	Diff MMF (%)
Enthesis	10.8 ( $p < 0.01$ )	–16.6 ( $p < 0.01$ )
Tendon	11.7 ( $p < 0.01$ )	–15.0 ( $p < 0.01$ )

Abbreviations: MMF, macromolecular proton fraction; PsA, psoriatic arthritis; UTE, ultrashort echo time.

respectively (Table 2). Excellent inter-reader reliability was observed with ICC values of 0.97 or higher for 3D UTE-T1, and MMF performed on all datasets. Excellent intra-reader reliability was observed with ICC values of 0.96 or higher performed on 10 randomly selected datasets.

Excellent repeatability was demonstrated with ICC values of 0.80 or higher and 0.90 or higher for T1 and MMF values, respectively.

As an exploratory investigation, a significant correlation was observed between MFF and T1 values (Spearman's  $R = -0.32$ ,  $p = 0.004$ ). The T1 and MMF relationship is shown in Figure S1.

## 4 | DISCUSSION

This study evaluated the Achilles tendon and entheses regions in patients with PsA and asymptomatic volunteers using 3D UTE-T1 and UTE-MT modeling techniques on a clinical 3-T scanner. We found significantly higher UTE-T1 values in the Achilles tendons and entheses of the PsA group compared with the asymptomatic volunteer group. Moreover, MMF from UTE-MT modeling showed significantly lower values in the Achilles tendon and the entheses of the PsA patients' group. Lower MMF values in patients agreed with previous preliminary results by Hodgson et al. that compared one patient with eight asymptomatic volunteers.<sup>18</sup>

In recent years, US and MRI have been the main modalities used to evaluate enthesitis in patients with PsA.<sup>5</sup> Earlier US studies demonstrated the potential presence of enthesitis in asymptomatic patients with psoriasis.<sup>24–26</sup> However, Gandjbakhch et al. have reported that US shows low reliability (29%) and responsiveness (defined as the ability of the tool to demonstrate a change in response to intervention) (19%) for evaluating enthesitis because of the lack of a standardized protocol.<sup>27</sup> Nevertheless, US can detect abnormalities of the entheses; it is operator dependent and is not routinely performed as a quantitative study.<sup>5</sup>

MRI plays a major role in the clinical diagnosis of enthesopathy. Conventional MRI sequences can show limited morphological changes in the Achilles tendon and surrounding tissues, such as the loss of the normal, flattened appearance, increased signal intensity, bone marrow edema, peri-enthesal inflammation, and distension of adjacent bursae.<sup>2,7,28</sup> Notably, semiquantitative grading systems have been developed for morphological and structural evaluations of the entheses, such as the Outcome Measures in Rheumatology (OMERACT) score, which uses gadolinium and postgadolinium T1-weighted and fat-suppressed T2-weighted images.<sup>9</sup> However, such semiquantitative morphological gradings focused mainly on the surrounding tissues instead of the entheses, which possess short T2s and show little or no signal with clinical sequences.<sup>29</sup> Quantitative diffusion-weighted imaging (DWI) acquired with routine sequences has shown promising results evaluating sacroiliac joints<sup>30–33</sup>; however, its use in entheses and tendons is probably limited because of the lack of signal in these short T2 tissues. To the best of our knowledge, DWI has not been investigated for tendon or enthesal evaluation in the peripheral joints.

2D- and 3D-UTE sequences offer promising results in morphological and quantitative evaluation of tissues with short T2,<sup>14,15</sup> but few studies have used these techniques to evaluate the entheses.<sup>13,16–18</sup> 3D-UTE sequences have drawn more attention from the research community as there are several theoretical advantages, including greater anatomic coverage, thinner slices, increased signal-to-noise ratio (SNR), and potentially reduced scan time, all facilitating clinical applications.<sup>14,19,34</sup> Among the reported 3D-UTE techniques,<sup>13,16</sup> UTE-MT modeling provides a magic angle insensitive biomarker in short T2 tissues<sup>14,19,35</sup> and has been investigated previously for the tendon,<sup>13,16,18,36–40</sup> ligament,<sup>41</sup> cartilage,<sup>42,43</sup> and bone<sup>42,44,45</sup> evaluations.

Chen et al. investigated UTE-T1 and MMF values ex vivo on five normal ankle specimens and reported lower T1 and MMF values compared with our study (T1 = 780 ± 55 ms and MMF = 13.9% ± 1.9% for entheses, T1 = 644 ± 22 ms and MMF = 18.0% ± 2.2% for tendon, respectively).<sup>16</sup> These are probably attributable to differences between the postmortem and in vivo conditions, including temperature (room temperature vs. body temperature).<sup>46</sup> Hodgson et al. investigated UTE-T1 and MMF (called the “bound proton fraction” in their study) values in Achilles tendons for eight volunteers compared with one PsA patient, but did not include the entheses regions. They used a 2D UTE radial sequence on a 1.5-T scanner and observed lower MMF and higher T1 values in the PsA patient compared with the volunteers.<sup>18</sup> Compared with our study, they reported lower T1 but comparable MMF values (T1 = 501 ± 65 ms and MMF = 21.0% ± 1.2% in the eight volunteers vs. T1 = 606 ms and MMF = 16.4% in the PsA patient), which can be attributed to the differences in the field strength, pulse sequences, MR acquisition parameters,

and sample. In this study we used the 3D-UTE-Cones sequence, which provides higher SNR, allows for faster acquisition, and reduces eddy current artifacts compared with the radial 2D-UTE sequence.<sup>13,35</sup>

Tbini et al. also calculated UTE- T1 maps for asymptomatic volunteers and patients with confirmed tendinopathy in the ankle.<sup>47</sup> They reported higher T1 values for patients ( $575 \pm 110$  vs.  $875 \pm 425$  ms for healthy volunteers and PsA patients, respectively), similar to our results. However, their reported low T1 values and large standard deviations can result from the heterogeneous and anatomically complex structure of the entheses. Chen et al. quantified T2\* and MTR measurements of the Achilles tendon and its enthesis on seven healthy volunteers and nine PsA patients with 3D-UTE-Cones on a 3-T scanner. They reported a significantly higher T2\*, while lower MTR, in both the tendon and enthesis of PsA patients.<sup>13</sup> As mentioned before, T2\* is sensitive to the magic angle effect,<sup>14</sup> while MTR values are difficult to interpret because of the dependence on the acquisition parameters.<sup>48–50</sup> It is essential to note that MTR cannot produce direct quantitative information on macromolecular and water protons present in tissues.<sup>19</sup>

Nevertheless, the current study was the first to examine UTE-MT modeling for in vivo enthesis evaluation, and we have also demonstrated its potential for distinguishing between patients with PsA and asymptomatic volunteers.<sup>14,19</sup>

This study had several limitations. First, the number of participants was low in this pilot investigation. Future investigations should be performed with a higher number of participants. Second, the PsA patients were older than the asymptomatic volunteers, and some of the observed differences between the groups may be confounded by age. Future investigations should be performed comparing PsA patients with age- and body mass index-matched control groups. Third, patients who might be under treatment for PsA were not identified to be excluded from the study. Future investigations should be performed evaluating PsA patients at baseline and after administration of treatments (e.g., biologics) to assess the responsiveness of the effects. Fourth, only UTE-T1 and MT modeling were used in this study; however, other promising UTE-MRI techniques, such as UTE-T1p, are recommended for tendons.<sup>51–53</sup> Finally, there are many components of the Achilles enthesis organ, including the fibrocartilages, bursa, and fat pad.<sup>54</sup> In our study, we chose to exclude these components, but variations in these structures may be relevant to disease processes and should be investigated in the future.

## 5 | CONCLUSIONS

Significantly higher UTE-T1 and lower MMF values were found in the entheses and tendons of PsA patients compared with asymptomatic volunteers. This study highlights the potential of UTE-T1 and UTE-MT modeling for quantitative evaluation of entheses and tendons in PsA patients.

## ACKNOWLEDGMENTS

The authors acknowledge grant support from the National Institutes of Health (R01AR075825, R01AR068987, R01AR062581, K01AR080257, R01AR079484, 5P30AR073761, and R01AR078877), U.S. Department of Veterans Affairs (I01CX001388, 1I01BX005952, and I01CX000625), and GE Healthcare.

## ORCID

Dina Moazamian  <https://orcid.org/0000-0002-8815-4535>

Jiyo S. Athertya  <https://orcid.org/0000-0002-0866-1052>

Alecio F. Lombardi  <https://orcid.org/0000-0002-6820-1779>

## REFERENCES

- Kaeley GS. Enthesitis in psoriatic arthritis (Part 2): imaging. *Rheumatology*. 2020;59(Suppl 1):i15–i20. doi:[10.1093/rheumatology/keaa040](https://doi.org/10.1093/rheumatology/keaa040)
- Barozzi L, Olivieri I, Matteis MD, Padula A, Pavlica P. Seronegative spondylarthropathies: imaging of spondylitis, enthesitis and dactylitis. *Eur J Radiol*. 1998;27:S12–S17. doi:[10.1016/S0720-048X\(98\)00037-0](https://doi.org/10.1016/S0720-048X(98)00037-0)
- Bakewell C, Aydin SZ, Ranganath VK, Eder L, Kaeley GS. Imaging techniques: options for the diagnosis and monitoring of treatment of enthesitis in psoriatic arthritis. *J Rheumatol*. 2020;47(7):973–982. doi:[10.3899/jrheum.190512](https://doi.org/10.3899/jrheum.190512)
- Baraliakos X, Sewerin P, de Miguel E, et al. Achilles tendon enthesitis evaluated by MRI assessments in patients with axial spondyloarthritis and psoriatic arthritis: a report of the methodology of the ACHILLES trial. *BMC Musculoskelet Disord*. 2020;21:767. doi:[10.1186/s12891-020-03775-4](https://doi.org/10.1186/s12891-020-03775-4)
- Mathew AJ, Coates LC, Danda D, Conaghan PG. Psoriatic arthritis: lessons from imaging studies and implications for therapy. *Expert Rev Clin Immunol*. 2017;13(2):133–142. doi:[10.1080/1744666X.2016.1215245](https://doi.org/10.1080/1744666X.2016.1215245)
- Aydin SZ, Tan AL, Hodgson R, et al. Comparison of ultrasonography and magnetic resonance imaging for the assessment of clinically defined knee enthesitis in spondyloarthritis. *Clin Exp Rheumatol*. 2013;31(6):933–936.
- Eshed I, Bollow M, McGonagle DG, et al. MRI of enthesitis of the appendicular skeleton in spondyloarthritis. *Ann Rheum Dis*. 2007;66(12):1553–1559. doi:[10.1136/ard.2007.070243](https://doi.org/10.1136/ard.2007.070243)
- Li WJ, Niu JL, Zhu L, Wang Y, An Y, Zhang SY. Comparison of the two magnetic resonance deartifact techniques in imaging of different porcelain-fused-to-metal crowns. *West China J Stomatol* 2019;37(1):66–69. doi:[10.7518/hxkq.2019.01.013](https://doi.org/10.7518/hxkq.2019.01.013)
- Mathew AJ, Østergaard M. Magnetic resonance imaging of enthesitis in spondyloarthritis, including psoriatic arthritis-status and recent advances. *Front Med (Lausanne)*. 2020;7:296. doi:[10.3389/fmed.2020.00296](https://doi.org/10.3389/fmed.2020.00296)

10. Afsahi AM, Sedaghat S, Moazamian D, et al. Articular cartilage assessment using ultrashort echo time MRI: a review. *Front Endocrinol.* 2022;13: 892961. doi:10.3389/fendo.2022.892961
11. Afsahi AM, Ma Y, Jang H, et al. Ultrashort echo time magnetic resonance imaging techniques: met and unmet needs in musculoskeletal imaging. *J Magn Reson Imaging.* 2022;55(6):1597-1612. doi:10.1002/jmri.28032
12. Xue YP, Ma YJ, Wu M, et al. Quantitative 3D ultrashort echo time magnetization transfer (3D UTE-MT) imaging for evaluation of knee cartilage degeneration in vivo. *J Magn Reson Imaging.* 2021;54(4):1294-1302. doi:10.1002/jmri.27659
13. Chen B, Zhao Y, Cheng X, et al. Three-dimensional ultrashort echo time cones (3D UTE-Cones) magnetic resonance imaging of entheses and tendons. *Magn Reson Imaging.* 2018;49:4-9. doi:10.1016/j.mri.2017.12.034
14. Ma YJ, Shao H, Du J, Chang EY. Ultrashort echo time magnetization transfer (UTE-MT) imaging and modeling: magic angle independent biomarkers of tissue properties. *NMR Biomed.* 2016;29(11):1546-1552. doi:10.1002/nbm.3609
15. Ma YJ, Lu X, Carl M, et al. Accurate T1 mapping of short T2 tissues using a three-dimensional ultrashort echo time cones actual flip angle imaging-variable repetition time (3D UTE-Cones AFI-VTR) method. *Magn Reson Med.* 2018;80(2):598-608. doi:10.1002/mrm.27066
16. Chen B, Cheng X, Dorthe EW, et al. Evaluation of normal cadaveric Achilles tendon and enthesis with ultrashort echo time (UTE) magnetic resonance imaging and indentation testing. *NMR Biomed.* 2019;32(1):e4034. doi:10.1002/nbm.4034
17. Hodgson RJ, Menon N, Grainger AJ, et al. Quantitative MRI measurements of the Achilles tendon in spondyloarthritis using ultrashort echo times. *Br J Radiol.* 2012;85(1015):e293-e299. doi:10.1259/bjr/13555456
18. Hodgson RJ, Evans R, Wright P, et al. Quantitative magnetization transfer ultrashort echo time imaging of the Achilles tendon. *Magn Reson Med.* 2011; 65(5):1372-1376. doi:10.1002/mrm.22715
19. Ma YJ, Chang EY, Carl M, Du J. Quantitative magnetization transfer ultrashort echo time imaging using a time-efficient 3D multispoke Cones sequence. *Magn Reson Med.* 2018;79(2):692-700. doi:10.1002/mrm.26716
20. Coates LC, Conaghan PG, Emery P, et al. Sensitivity and specificity of the classification of psoriatic arthritis criteria in early psoriatic arthritis. *Arthritis Rheum.* 2012;64(10):3150-3155. doi:10.1002/art.34536
21. Taylor W, Gladman D, Helliwell P, et al. Classification criteria for psoriatic arthritis: development of new criteria from a large international study. *Arthritis Rheum.* 2006;54(8):2665-2673. doi:10.1002/art.21972
22. Klein S, Staring M, Murphy K, Viergever MA, Pluim JPW. elastix: a toolbox for intensity-based medical image registration. *IEEE Trans Med Imaging.* 2010;29(1):196-205. doi:10.1109/TMI.2009.2035616
23. Ma YJ, Zhao W, Wan L, et al. Whole knee joint T1 values measured in vivo at 3T by combined 3D ultrashort echo time cones actual flip angle and variable flip angle methods. *Magn Reson Med.* 2019;81(3):1634-1644. doi:10.1002/mrm.27510
24. De Filippis LG, Caliri A, Lo Gullo R, et al. Ultrasonography in the early diagnosis of psoriasis-associated enthesopathy. *Int J Tissue React.* 2005;27(4): 159-162.
25. Özçakar L, Çetin A, İnanici F, Kaymak B, Gürer CK, Kölemen F. Ultrasonographical evaluation of the Achilles' tendon in psoriasis patients. *Int J Dermatol.* 2005;44(11):930-932. doi:10.1111/j.1365-4632.2004.02235.x
26. Gisondi P, Tinazzi I, El-Dalati G, et al. Lower limb enthesopathy in patients with psoriasis without clinical signs of arthropathy: a hospital-based case-control study. *Ann Rheum Dis.* 2008;67(1):26-30. doi:10.1136/ard.2007.075101
27. Gandjbakhch F, Terslev L, Joshua F, et al. Ultrasound in the evaluation of enthesitis: status and perspectives. *Arthritis Res Ther.* 2011;13(6):R188. doi:10.1186/ar3516
28. McGonagle D, Marzo-Ortega H, O'Connor P, et al. The role of biomechanical factors and HLA-B27 in magnetic resonance imaging-determined bone changes in plantar fascia enthesopathy. *Arthritis Rheum.* 2002;46(2):489-493. doi:10.1002/art.10125
29. Benjamin M, Bydder GM. Magnetic resonance imaging of entheses using ultrashort TE (UTE) pulse sequences. *J Magn Reson Imaging.* 2007;25(2):381-389. doi:10.1002/jmri.20825
30. Vendhan K, Bray TJP, Atkinson D, et al. A diffusion-based quantification technique for assessment of sacroiliitis in adolescents with enthesitis-related arthritis. *Br J Radiol.* 2016;89(1059):20150775. doi:10.1259/bjr.20150775
31. Gezmis E, Donmez FY, Agildere M. Diagnosis of early sacroiliitis in seronegative spondyloarthropathies by DWI and correlation of clinical and laboratory findings with ADC values. *Eur J Radiol.* 2013;82(12):2316-2321. doi:10.1016/j.ejrad.2013.08.032
32. Lecouvet FE, Vander Maren N, Collette L, et al. Whole body MRI in spondyloarthritis (SpA): Preliminary results suggest that DWI outperforms STIR for lesion detection. *Eur Radiol.* 2018;28(10):4163-4173. doi:10.1007/s00330-018-5377-3
33. Ran J, Morelli JN, Xie R, et al. Role for imaging in spondyloarthritis. *Q J Nucl Med Mol Imaging.* 2017;61(3):271-282.
34. Carl M, Bydder GM, Du J. UTE imaging with simultaneous water and fat signal suppression using a time-efficient multispoke inversion recovery pulse sequence. *Magn Reson Med.* 2016;76(2):577-582. doi:10.1002/mrm.25823
35. Springer F, Martirosian P, Machann J, Schwenzler NF, Claussen CD, Schick F. Magnetization transfer contrast imaging in bovine and human cortical bone applying an ultrashort echo time sequence at 3 Tesla. *Magn Reson Med.* 2009;61(5):1040-1048. doi:10.1002/mrm.21866
36. Ashir A, Ma Y, Jerban S, et al. Rotator cuff tendon assessment in symptomatic and control groups using quantitative magnetic resonance imaging. *J Magn Reson Imaging.* 2020;52(3):864-872. doi:10.1002/jmri.27115
37. Jerban S, Ma Y, Afsahi AM, et al. Lower Macromolecular Content in Tendons of Female Patients with Osteoporosis versus Patients with Osteopenia Detected by Ultrashort Echo Time (UTE) MRI. *Diagnostics (Basel).* 2022;12(5):1061. doi:10.3390/diagnostics12051061
38. Jerban S, Ma Y, Alenezi S, et al. Ultrashort echo time (UTE) MRI porosity index (PI) and suppression ratio (SR) correlate with the cortical bone microstructural and mechanical properties: Ex vivo study. *Bone.* 2023;169:116676. doi:10.1016/j.bone.2023.116676
39. Zhu Y, Cheng X, Ma Y, et al. Rotator cuff tendon assessment using magic-angle insensitive 3D ultrashort echo time cones magnetization transfer (UTE-Cones-MT) imaging and modeling with histological correlation. *J Magn Reson Imaging.* 2018;48(1):160-168. doi:10.1002/jmri.25914
40. Fang Y, Zhu D, Wu W, Yu W, Li S, Ma YJ. Assessment of Achilles tendon changes after long-distance running using ultrashort echo time magnetization transfer MR imaging. *J Magn Reson Imaging.* 2022;56(3):814-823. doi:10.1002/jmri.28072
41. Jerban S, Hananouchi T, Ma Y, et al. Correlation between the elastic modulus of anterior cruciate ligament (ACL) and quantitative ultrashort echo time (UTE) magnetic resonance imaging. *J Orthop Res Off Publ Orthop Res Soc.* 2022;40(10):2330-2339. doi:10.1002/jor.25266



42. Jerban S, Kasibhatla A, Ma Y, et al. Detecting articular cartilage and meniscus deformation effects using magnetization transfer ultrashort echo time (MT-UTE) modeling during mechanical load application: ex vivo feasibility study. *Cartilage*. 2021;13(1\_suppl):665S-673S. doi:[10.1177/1947603520976771](https://doi.org/10.1177/1947603520976771)
43. Namiraniyan B, Jerban S, Ma Y, et al. Assessment of mechanical properties of articular cartilage with quantitative three-dimensional ultrashort echo time (UTE) cones magnetic resonance imaging. *J Biomech*. 2020;113:110085. doi:[10.1016/j.jbiomech.2020.110085](https://doi.org/10.1016/j.jbiomech.2020.110085)
44. Jerban S, Ma Y, Wan L, et al. Collagen proton fraction from ultrashort echo time magnetization transfer (UTE-MT) MRI modelling correlates significantly with cortical bone porosity measured with micro-computed tomography ( $\mu$ CT). *NMR Biomed*. 2019;32(2):e4045. doi:[10.1002/nbm.4045](https://doi.org/10.1002/nbm.4045)
45. Jerban S, Ma Y, Nazaran A, et al. Detecting stress injury (fatigue fracture) in fibular cortical bone using quantitative ultrashort echo time-magnetization transfer (UTE-MT): an ex vivo study. *NMR Biomed*. 2018;31(11):e3994. doi:[10.1002/nbm.3994](https://doi.org/10.1002/nbm.3994)
46. Jerban S, Szevenyi N, Ma Y, et al. (ISMRM 2019) Ultrashort echo time MRI (UTE-MRI) quantifications of cortical bone varied between scans at room temperature and body temperature.
47. Tbini Z, Mars M, Bouaziz M. T1 relaxation time of Achilles Tendon at 3 Tesla with special reference to relevant clinical score: a preliminary study. *Curr Med Imaging Rev*. 2020;16(2):164-173. doi:[10.2174/1573405615666181205130816](https://doi.org/10.2174/1573405615666181205130816)
48. Yang J, Shao H, Ma Y, et al. Quantitative ultrashort echo time magnetization transfer (UTE-MT) for diagnosis of early cartilage degeneration: comparison with UTE-T2\* and T2 mapping. *Quant Imaging Med Surg*. 2020;10(1):171-183. doi:[10.21037/qims.2019.12.04](https://doi.org/10.21037/qims.2019.12.04)
49. Jerban S, Ma Y, Dorthe EW, et al. Assessing cortical bone mechanical properties using collagen proton fraction from ultrashort echo time magnetization transfer (UTE-MT) MRI modeling. *Bone Rep*. 2019;11:100220. doi:[10.1016/j.bonr.2019.100220](https://doi.org/10.1016/j.bonr.2019.100220)
50. Sinclair CDJ, Samson RS, Thomas DL, et al. Quantitative magnetization transfer in in vivo healthy human skeletal muscle at 3 T. *Magn Reson Med*. 2010;64(6):1739-1748. doi:[10.1002/mrm.22562](https://doi.org/10.1002/mrm.22562)
51. Ma YJ, Carl M, Shao H, Tadros AS, Chang EY, Du J. Three-dimensional ultrashort echo time cones T1p (3D UTE-cones-T1p) imaging. *NMR Biomed*. 2017;30(6):e3709. doi:[10.1002/nbm.3709](https://doi.org/10.1002/nbm.3709)
52. Ma YJ, Carl M, Searleman A, Lu X, Chang EY, Du J. 3D adiabatic T(1p) prepared ultrashort echo time cones sequence for whole knee imaging. *Magn Reson Med*. 2018;80(4):1429-1439. doi:[10.1002/mrm.27131](https://doi.org/10.1002/mrm.27131)
53. Wang N, Xia Y. Anisotropic analysis of multi-component T2 and T1p relaxations in Achilles tendon by NMR spectroscopy and microscopic MRI. *J Magn Reson Imaging*. 2013;38(3):625-633. doi:[10.1002/jmri.24012](https://doi.org/10.1002/jmri.24012)
54. McGonagle D, Lories RJ, Tan AL, Benjamin M. The concept of a "synovio-entheseal complex" and its implications for understanding joint inflammation and damage in psoriatic arthritis and beyond. *Arthritis Rheum*. 2007;56(8):2482-2491. doi:[10.1002/art.22758](https://doi.org/10.1002/art.22758)

## SUPPORTING INFORMATION

Additional supporting information can be found online in the Supporting Information section at the end of this article.

**How to cite this article:** Moazamian D, Athertya JS, Dwek S, et al. Achilles tendon and entheses assessment using ultrashort echo time magnetic resonance imaging (UTE-MRI) T1 and magnetization transfer (MT) modeling in psoriatic arthritis. *NMR in Biomedicine*. 2024; 37(1):e5040. doi:[10.1002/nbm.5040](https://doi.org/10.1002/nbm.5040)